

EXPERIMENTAL AND COMPUTATIONAL VISUALIZATION AND FREQUENCY MEASUREMENTS OF THE JET OSCILLATION INSIDE A FLUIDIC OSCILLATOR

O. Uzol, C. Camci

Abstract The jet oscillation inside a fluidic oscillator is investigated in detail in order to obtain more information about the physical mechanisms that drive the jet oscillation. Particle Image Velocimetry measurements are conducted inside the oscillation chamber of the fluidic oscillator in order to visualize and measure the frequency of the jet oscillation. A transparent afterbody allowed laser illumination of the oscillation chamber. The experiments are conducted for a low jet exit Reynolds number of 321, based on the maximum velocity and the nozzle width at the jet exit plane. Computational simulations of the flow field inside the oscillation chamber are obtained by solving two-dimensional, incompressible and unsteady Navier-Stokes equations for the same throat Reynolds number and using a finite element methodology. The flow field is assumed to be laminar and constant viscosity. The jet oscillation frequency obtained from the computational simulations is underpredicted but still in close agreement with the measured PIV frequency. The computational simulations also revealed the formation of a pressure gradient across the jet as it is deflected from the symmetry position. This is one of the main driving mechanisms of the jet oscillation. The variation of the jet oscillation frequency with throat Reynolds number is also determined by single sensor hot-wire measurements inside the oscillation chamber.

1 Introduction

Fluidic oscillators have been used as flow meters for mass flow rate measurement purposes. These are compact devices with no moving parts, simplicity of construction and low cost. The main operating principle of the fluidic oscillator is the generation of self-induced and sustained oscillations of the flow that has a frequency which is proportional to the mass flow rate. Most of the fluidic oscillator designs make use of an oscillating jet inside the device which is created by fluid mechanical interactions.

Many different design concepts are investigated and implemented for the creation of the jet oscillation. Parry et al (1991) investigated a target fluidic oscillator in which the jet oscillation is created due to the interaction of a planar jet with a bluff body, called target. The principle of operation of a similar target fluidic oscillator is explained in detail in Boucher and Mazharoglu (1988). Mansy and Williams (1989) investigated a trapped vortex pair oscillator. The jet oscillation principle for this device was mentioned to be dependent upon the formation of two counter rotating vortices that are trapped in a convergent channel. Bauer (1981) proposed another kind of fluidic oscillator which creates a jet oscillation due to the impingement of the jet on a concave wall. More recently, similar oscillators which use the same physical phenomenon have been proposed by Huang (1995) and Huang and Hocquet (1995). Fluidic oscillators have also been proposed as heat transfer augmentation devices. A pin fin cooling device called the 'oscillator fin' is investigated in detail by Uzol (2000) and Uzol and Camci (1998) as an alternative to circular pin fins. This concept is also based on Bauer's (1981) fluidic oscillator.

In this study the jet oscillation inside the fluidic oscillator proposed by Bauer (1981) is investigated in detail in order to obtain more information about the physical mechanisms that drive the jet oscillation inside the oscillation chamber. The variation of the jet oscillation frequency with Reynolds number is determined. Both an experimental and a computational study is performed. Particle Image Velocimetry measurements and visualizations are conducted inside the oscillation chamber of the fluidic oscillator. The jet oscillation frequency is measured by hot-wire anemometry. The computational simulations are performed to obtain detailed flow physics of this device.

O. Uzol, The Pennsylvania State University, University Park, PA, USA (Currently at The Johns Hopkins University, Baltimore, MD, USA)

C. Camci, The Pennsylvania State University, University Park, PA, USA

Correspondence to:
Dr. Oguz Uzol, Department of Mechanical Engineering, 200 Latrobe Hall, The Johns Hopkins University, 3400 N. Charles Str., Baltimore, MD, 21218, USA. E-mail: uzol@jhu.edu

2
Fluidic Oscillator Geometry and Operation

The fluidic oscillator geometry consists of three separate members (Fig. 1). Two front members which are of elliptical cross-section are placed transversely across the passage with the major axis of the ellipse parallel to the flow direction. These two members form a tapering nozzle which is used to create a jet between them. The downstream ends of the front members are defined as downstream facing cusps which will be used for directing the oscillating jet into the flow. The third member which receives the jet from the nozzle is called the afterbody and has an upstream facing U shaped geometry. The concave wall inside the afterbody where the jet impinges and the jet oscillation occurs is called the oscillation chamber. The relative dimensions of the oscillator fin are also given in Fig. 1.

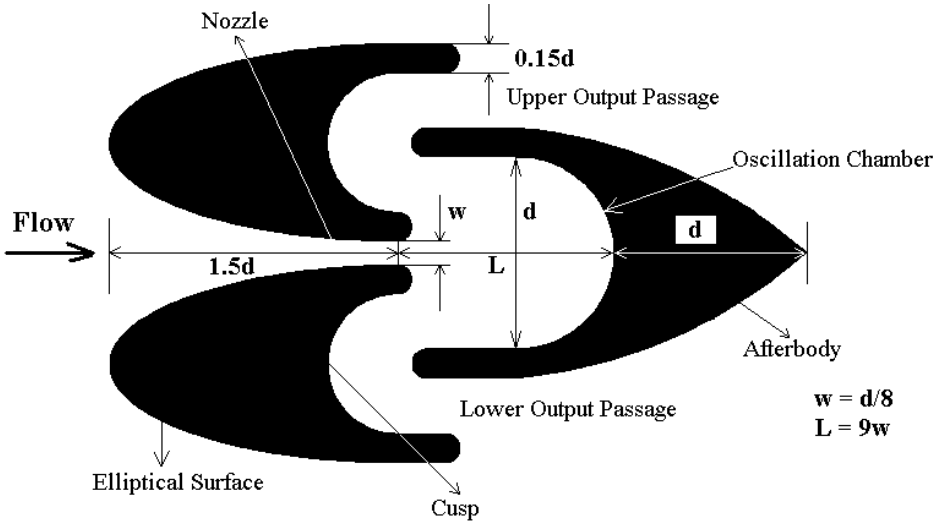

Fig: 1. Fluidic Oscillator Geometry

During the operation of the oscillator fin, the jet coming from the nozzle impinges against the wall of the oscillation chamber and splits into two oppositely directed flows while generating two counter rotating vortices with equal magnitude of vorticity. At the very first instant the flow field inside the oscillation chamber is symmetrical. The oppositely directed flows on the upper and lower side of the jet have the same amount of mass flow rate and they exit from the upper and lower output passages, respectively. However this symmetrical layout is very unstable and any minute asymmetry in the domain results in the deflection of the jet towards one of the sides (upper or lower) and therefore destroying the symmetry. This instantly starts the inherently unsteady and periodic large scale oscillation of the jet impinging up on the concave wall. As the jet created between the two front members is swept back and forth inside the oscillation chamber, alternating flow pulses are formed and directed by cusps into the main flow.

3
PIV Measurements and Visualization

Experimental Setup

A flow visualization study inside the oscillation chamber of the fluidic oscillator is performed using particle image velocimetry to demonstrate the existence of the jet oscillation and to get some more insight to the fluidic oscillator operation. For this purpose a fluidic oscillator model with an afterbody constructed using transparent material is used in order to be able to illuminate the oscillation chamber. The experiments are conducted in the Low Speed Heat Transfer Facility at the Pennsylvania State University. This is an open loop wind tunnel with an axial air blower, a diffuser with multiple screens, a plenum chamber, a high area ratio circular nozzle, a circular to rectangular transition duct, the test section and a diffuser. The test section is a 127 cm long straight rectangular duct made out of 1.27 cm thick clear acrylic and has a 36.67 cm x 7.62 cm cross-section. Figure 2 shows the experimental facility and more details about the facility can be found in Uzol and Camci() and Uzol(). The flow field is illuminated illuminated from the bottom of the tunnel test section by a double-cavity frequency-doubled pulsating Nd:YAG laser sheet which has an emitted radiation wavelength of 532 nm and 50 mJ per pulse energy level. The seeding is done using fog particles with particle sizes varying from 0.25 μm to 60 μm. Images of the flow field are captured using a 1k x 1k Kodak Megaplus ES 1.0 cross-correlation CCD camera which is fully synchronized with the

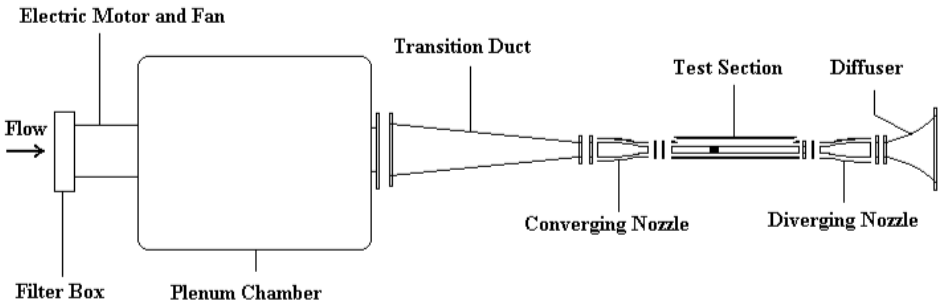

Fig: 2. Low Speed Heat Transfer Research Facility

pulsating laser sheet. In order to be able to capture different phases of the jet oscillation, the experiments are conducted at a low free stream Reynolds number of 4048 calculated using the free stream velocity and the width of the oscillator fin. The corresponding Reynolds number at the jet exit plane (nozzle) inside the oscillator fin is 321, calculated using the maximum velocity and the nozzle width at that plane. Running at low Reynolds number would yield a low oscillation frequency which could be captured with the CCD camera of the PIV system which has a maximum frequency response of 15 Hz (maximum frame rate of the camera). The PIV measurement setup is iluustrated in Fig. 3.

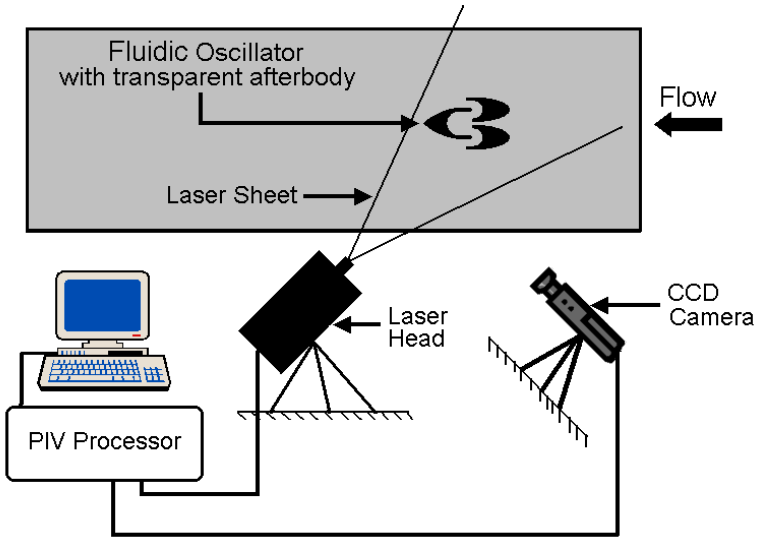

Fig. 3 PIV Measurement Setup

Results

The PIV image sequences and velocity vectors showing the jet oscillation inside the fluidic oscillator is given in Fig. 4. It is observed that the jet oscillation inside the chamber is strongly periodic. While the jet is continuously fed from the nozzle, it oscillates between the lower and upper sidewalls of the oscillation chamber. One oscillation cycle can be defined as the jet starting from the position that it is attached to the bottom sidewall, continues to deflect and attaches itself to the upper sidewall and finally comes back to the position where it started, i.e. back to the lower sidewall of the oscillation chamber. It is observed that this cycle repeats itself after 10 PIV images. The PIV image and velocity vector sequences in Fig. 4 are samples chosen to illustrate the oscillation. Knowing the time interval

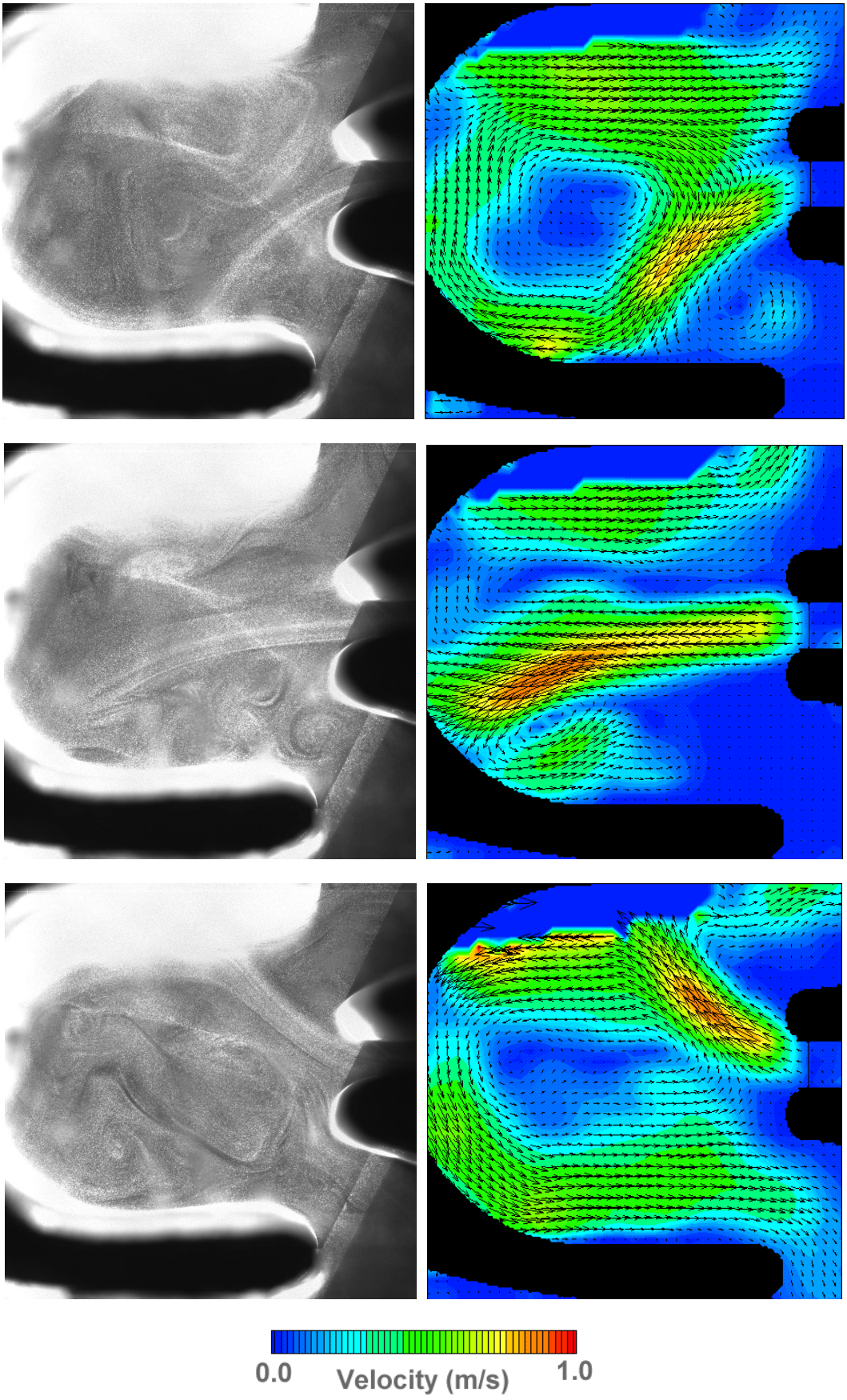

Fig: 4. PIV Images and Velocity Contours inside the Oscillation Chamber

between each image is 67 ms, it is possible to obtain the period of this cycle. The period of the oscillation cycle is found as 0.603 s which corresponds to an oscillation frequency of 1.658 Hz at the current nozzle exit Reynolds number. Formation and the unsteady interaction of the two vortical structures at the upper and lower sides of the jet are revealed. The unsteady interaction of these two vortices is one of the main driving mechanism of the jet oscillation.

4
Computational Simulations of the Jet Oscillation

Computational simulations of the flow field inside the oscillation chamber of the oscillator fin are performed in order to better understand the physics of the jet oscillation. The simulations are obtained by solving two dimensional, isothermal, incompressible and transient Navier Stokes equations. The flow field is assumed to be laminar and constant viscosity. Hence the governing equations of the flow field are,

$$u_{i,i} = 0 \tag{1}$$

$$\rho\left(\frac{\partial u_i}{\partial t} + u_j u_{i,j}\right) = -P_{,i} + \tau_{ij,j} \tag{2}$$

where,

$$\tau_{ij} = \mu\left(u_{i,j} + u_{j,i}\right) \tag{3}$$

A finite element based fluid dynamics analysis package FIDAP ()is used to solve the governing equations. The flow domain is discretized by nine-node quadrilateral elements which give a biquadratic velocity and bilinear pressure variation within each element. The reduced formulation for pressure, known as the 'penalty method' is used. When this method is implemented the continuity equation is discarded and the pressure is eliminated from the momentum equation using,

$$P = -\left(\frac{1}{\varepsilon}\right)\nabla \cdot u \tag{4}$$

where ε is the penalty parameter. Implicit backward Euler temporal formulation with a variable time increment is used for time integration. The variable time step size is controlled by a maximum local relative time truncation error of 0.1%. At each time step the equations are solved using quasi-Newton method with full reformulation on the first iteration only. The computations are performed for a jet exit Reynolds number (Re_{thr}) of 321 at which the PIV flow visualization study is performed. Velocity components are specified zero on the walls in order to satisfy the no-slip condition. Since imposing an inlet boundary condition at the jet exit plane would prevent the velocity vector to change direction at that location, it would not be possible to initiate the jet oscillation inside the oscillation chamber. Instead the flow field is started upstream and the inlet boundary conditions are imposed here, so that the velocity vector at the jet exit plane could freely change direction. A uniform steady profile is imposed here such that the velocity at the throat would give the desired throat Reynolds number. The y component of the velocity is specified as zero at this location. No boundary conditions are explicitly imposed for velocity components at the outflow boundary. The specific form of the finite element solution procedure results in zero streamwise gradients for these variables at the exit plane. The unsteady solution is started from zero velocity initial fields. The computational mesh is illustrated in Fig. 4. 936 second order nine-node quadrilateral elements are created which resulted in 3247 nodes.

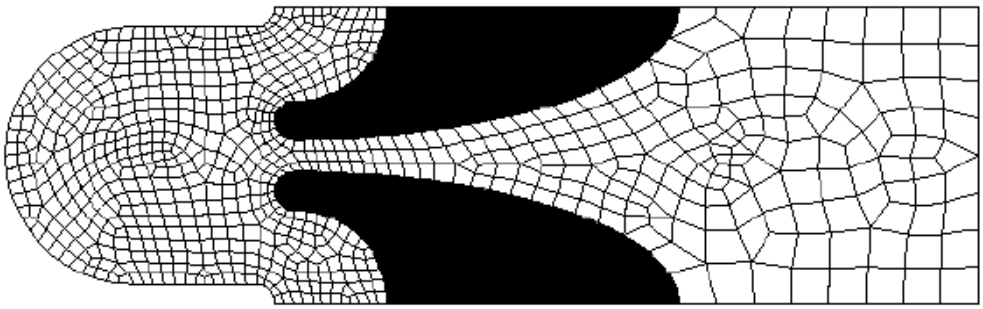

Fig: 5. Computational Mesh used for Jet Oscillation Simulations

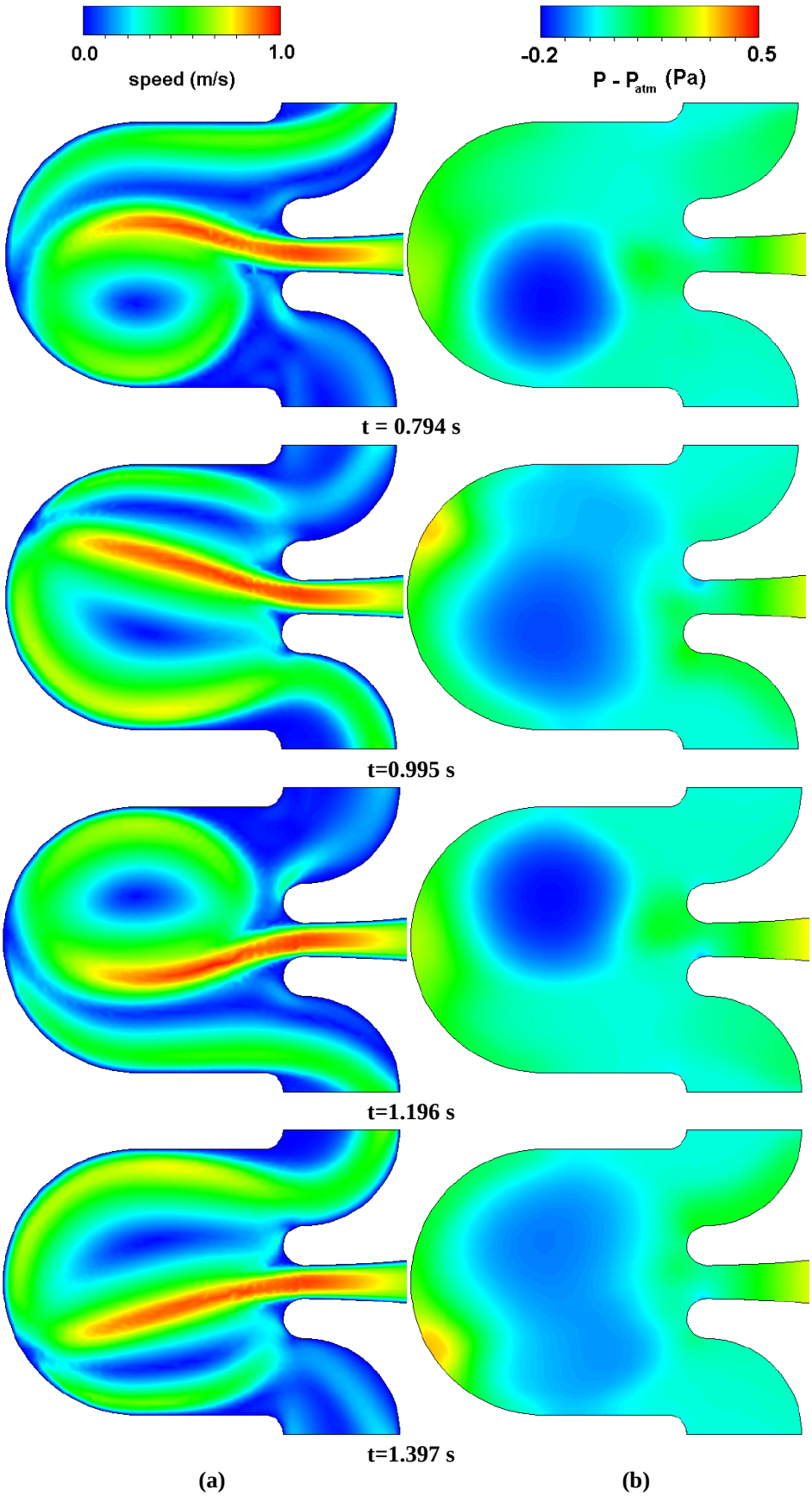

Fig: 6. Computed (a) Velocity (b) Pressure Contours inside the Oscillation Chamber

It is observed from the computational results that during the first 86 time steps (0.381 s) of the computation, the jet starts to form and slowly reach and impinge upon the concave wall of the oscillation chamber, since the unsteady computations are started from a zero initial velocity field. The two vortices on either side of the jet are also slowly formed during this time period. The flow field up to this point is fully symmetrical. However after this time step the jet starts to deflect from this symmetrical position and a periodic oscillation is achieved afterwards. It is found that one jet oscillation cycle is completed in 12 frames in computational simulations whereas it was completed in 10 frames in the PIV visualization experiments. This shows that for the same Reynolds number and flow conditions, the frequency of the jet oscillation is underpredicted in the computations. Nevertheless, it was possible to obtain more information about the flow physics and the jet oscillation mechanism from the computational results. The formation and the interaction of the two counter rotating vortices on either side of the jet are visualized by the computations. It is also observed that the maximum jet deflection angle is much lower than the deflection angle observed from the PIV flow visualizations. The computed speed and pressure contours during one cycle of oscillation inside the oscillation chamber are illustrated in Fig. 6. As the jet deflects and starts to move towards the upper output passage, the lower vortex starts to get bigger and the pressure inside the vortex starts to decrease. When the jet reaches its maximum deflection point, a pressure gradient is created across the jet which starts to pull the jet towards the symmetry line. However the mutual unsteady interaction of the vortices inside the oscillation chamber keeps the jet oscillating between the upper and lower side walls.

The jet oscillation frequency as defined in the PIV flow visualization study can also be determined from the results of the computational simulations. Fig. 7a shows the time history of static pressure at a control point 15 mm downstream of the jet exit plane and right on the symmetry line. The periodic variation of the pressure is clearly visible from this figure. An FFT analysis of the pressure history (Fig. 7b) gives a dominant frequency at 2.68 Hz. However during one oscillation cycle the jet sweeps the control point twice. Therefore the actual jet oscillation frequency, as defined in the PIV flow visualization study, is half of this frequency which is 1.34 Hz which is underpredicted but still in close agreement with the frequency value measured in PIV experiments (1.658 Hz) for this Reynolds number. It was not possible to obtain and initiate the jet oscillation process for higher Reynolds numbers due to the need to increase the effect of the 'balancing tensor diffusivity' method of upwinding offered in FIDAP to obtain stable solutions at high Reynolds numbers. Increasing the effect of the upwinding terms for high Reynolds numbers results in an increase in false diffusion created by the upwinding scheme and hence supresses the jet oscillation.

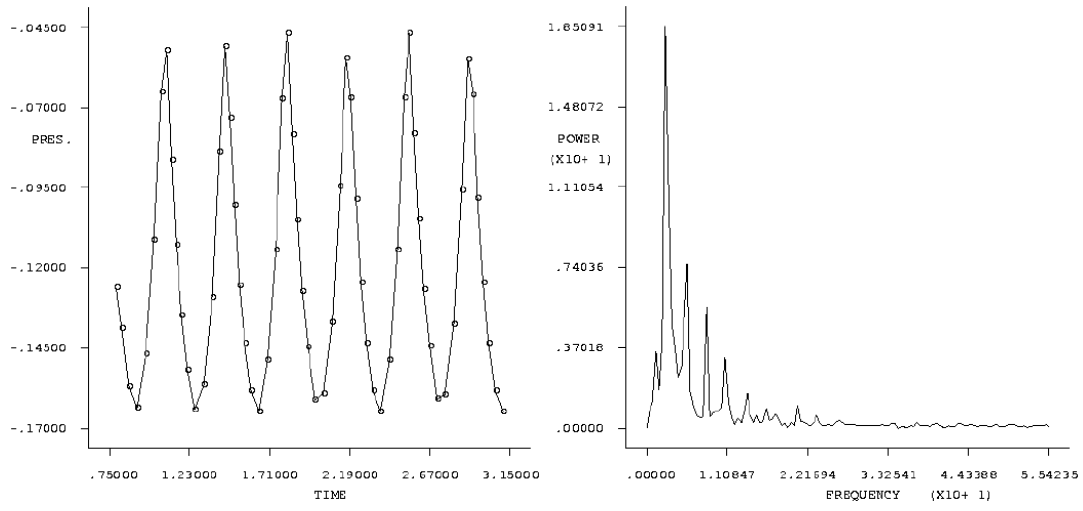

(a) (b)

Fig: 7. (a) Time History of Pressure (b) FFT of the Computed Pressure Time History

5
Jet Oscillation Frequency Measurements

After observing the existence and the physical mechanisms of the jet oscillation inside the oscillation chamber, an experimental study is conducted to investigate the variation of the jet oscillation frequency with throat and free stream Reynolds numbers. For this purpose the oscillator fin model is placed inside the test section of the Low Speed Heat Transfer Research Facility and a single sensor hotwire probe is placed inside the oscillation chamber 15 mm downstream of the jet exit plane as shown in Fig. 8. The single sensor hotwire probe is operated through a DISA type 55M01 single sensor hotwire anemometer system. The signal from the hotwire anemometer is first

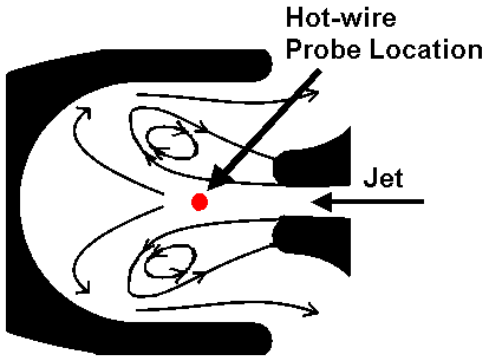

Fig: 8. Hot-wire Probe Location for Frequency Measurements

passed through a low pass filter for anti-aliasing purposes and to be able to capture the low frequency jet oscillations. The filtered signal is then fed into a digital oscilloscope and the time signature of the signal is observed for different Reynolds numbers. An online FFT analysis of the signal is also performed to capture the jet oscillation frequency which is appeared as a dominant frequency in the FFT analysis.

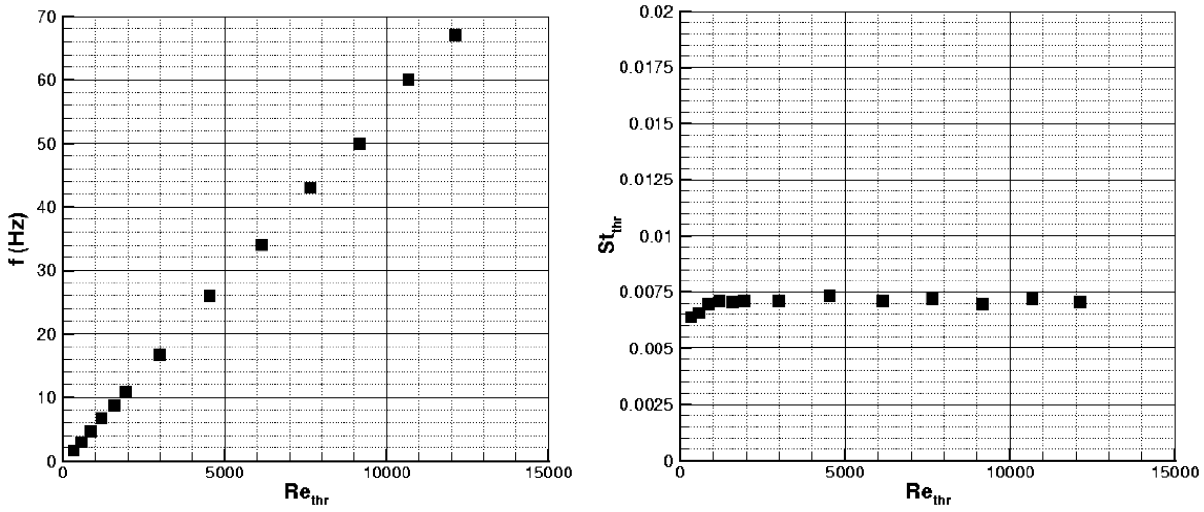

(a) (b)

Fig: 9. Variation of (a) Jet Oscillation Frequency (b) Throat Stouhal Number with Throat Reynols Number

The variation of the jet oscillation frequency with the throat Reynolds number is given in Fig. 9a. It is observed that the frequency varies linearly in a wide range of Reynolds numbers. The measured jet oscillation frequency for a throat Reynolds number 321, at which the PIV flow visualization study is performed, is 1.6 Hz which is in agreement with the frequency observed from the PIV flow visualization study. Fig. 9b shows the Strouhal number variation with throat Reynolds number. It is observed that the variation is almost constant in a wide Reynolds number range. The free stream Reynolds numbers are calculated using the velocity measured at the inlet of the test section and the width of the oscillator fin. The throat Strouhal numbers are calculated using the throat width and the velocity measured at the throat location.

6 Conclusions

The operation of a fluidic oscillator and the jet oscillation mechanism inside it have been studied in detail. It is seen that the jet oscillation is an inherently unsteady phenomenon and mainly driven by the unsteady motion of two counter-rotating vortices on either side of the jet. The concavity of the wall of the oscillation chamber upon which the jet impinges also plays an important role in the jet oscillation process. Unsteady variation of the pressure gradient across the jet, which is essentially due to the changing sizes of the counter-rotating vortices, continuously keeps the jet oscillating back and forth inside the oscillation chamber. The existence of this jet oscillation is visualized experimentally using Particle Image Velocimetry. The formation and the unsteady interaction of the two

vortical structures are also visualized. Computational simulations of the jet oscillation revealed the details about the formation process of the transverse pressure gradient across the jet. The jet oscillation frequency obtained from the PIV measurements and computational simulations are in close agreement. The variation of the jet oscillation frequency with the free stream Reynolds number is also determined experimentally. It is seen that the frequency varies linearly in a wide range of Reynolds numbers and that produces an almost constant Strouhal number variation in the Reynolds number range.

References

Bauer P. (1980), Fluidic Oscillator and Spray Forming Output Chamber, United States Patent No. 4,184,636

Bauer P. (1981) Fluidic Oscillator Flowmeter, United States Patent No. 4,244,230

Boucher R.F.; Mazharoglu C. (1988), Low Reynolds Number Fluidic Flowmetering, J. Phys. E. Sci. Instrum., Vol. 21, pp. 977-989

Huang B.T. (1995), Flowmeter Having a Fluidic Oscillator, United States Patent No. 5,396,809

Huang B.T.; Hocquet J (1995), Fluidic Oscillator, United States Patent No. 5,396,808

Mansy H.; Williams D.R. (1989), An Experimental and Numerical Study of Trapped Vortex Pair Fluidic Flowmeter, ASME FED Forum on Turbulent Flows, Vol. 76, pp. 35-39

Parry A. J.; Chiwanga S.G.; Kalsi H.S.; Jepson P. (1991), Numerical and Experimental Visualization of Flow Through a Target Fluidic Oscillator, ASME FED Experimental and Numerical Flow Visualization, Vol.128, pp. 327-334

Uzol O.; Camci C. (1998), Oscillator Fin as a Novel Heat Transfer Augmentation Device for Gas Turbine Blade Cooling Applications, Proceedings of ASME Turbo Expo 1998, Stockholm, Sweden

Uzol O.; (2000), Novel Concepts and Geometries as Alternatives to Conventional Circular Pin Fins for Gas Turbine Blade Cooling Applications, Ph.D. Thesis, Pennsylvania State University, University Park, PA, USA.